

NUMERICAL PASSAGE FROM SYSTEMS OF CONSERVATION LAWS TO HAMILTON–JACOBI EQUATIONS, AND RELAXATION SCHEMES*

SHI JIN[†] AND ZHOUPING XIN[‡]

Dedicated to Ami Harten

Abstract. In this paper we study the numerical transition from a Hamilton–Jacobi (H–J) equation to its associated system of conservation laws in arbitrary space dimensions. We first study how, in a very generic setting, one can recover the viscosity solutions of the H–J equation using the numerical solutions to the system of conservation laws. We then introduce a simple, second-order relaxation scheme to solve the underlying weakly hyperbolic system of conservation laws.

Key words. Hamilton–Jacobi equations, weakly hyperbolic system of conservation laws, shock capturing methods, numerical viscosity, relaxation schemes

AMS subject classifications. 35L40, 65M05, 35F25

PII. S0036142996314366

1. Introduction. Hamilton–Jacobi (H–J) equations arise in a variety of applications, such as optimal control, game theory, geometric optics, and front propagation. In this paper we study several numerical issues associated with a general H–J equation in n space dimensions:

$$(1.1) \quad \partial_t u + H(\nabla u) = 0.$$

Here ∇ is the gradient with respect to $\mathbf{x} = (x_1, \dots, x_n)$, defined by $\nabla = (\partial_{x_1}, \dots, \partial_{x_n})$, unless otherwise specified. It is known that this equation has a close relation with a system of conservation laws. Let $\mathbf{p} = (p_1, \dots, p_n)$, where

$$(1.2) \quad \mathbf{p} = \nabla u \quad \text{or} \quad p_1 = \partial_{x_1} u, \dots, \quad p_n = \partial_{x_n} u;$$

then \mathbf{p} formally solves the n -dimensional system of conservation laws

$$(1.3a) \quad \partial_t \mathbf{p} + \nabla H(\mathbf{p}) = 0.$$

Clearly, if \mathbf{p} is known, then one may recover u from \mathbf{p} by integrating the ordinary differential equation

$$(1.3b) \quad \partial_t u + H(\mathbf{p}) = 0.$$

We would like to point out that system (1.3) is only *weakly* hyperbolic in high dimension ($n \geq 2$) in that there is no complete set of eigenvectors. Thus it is not well posed in the strong sense.

*Received by the editors December 30, 1996; accepted for publication (in revised form) January 12, 1998; published electronically November 13, 1998.

<http://www.siam.org/journals/sinum/35-6/31436.html>

[†]School of Mathematics, Georgia Institute of Technology, Atlanta, GA 30332 (jin@math.gatech.edu). The research of this author was partially supported by NSF grants DMS-9404157 and DMS-9704957.

[‡]Courant Institute, New York University, New York, NY 10012 (xinz@cims.nyu.edu). The research of this author was partially supported by NSF grant DMS 9600137 and DOE grant DO-FG02-88ER-25053.

Understanding the relation between (1.1) and (1.3), both theoretically and numerically, has been a rich research subject. Theoretically, one gains a better understanding of the solution to (1.1) by knowing (1.3) has been studied intensively in the past several decades. For example, it is known that the generic solutions to the system of conservation laws develop shocks (discontinuous solutions) in finite time even if the initial data are smooth [21]. The relation (1.2) suggests that the solution of u will develop a cusp where \mathbf{p} , the derivative of u , is discontinuous. The concept of weak entropy solutions, in the sense that they are limits of the solutions to the corresponding viscous regularization problems, was introduced to obtain a unique weak solution for both systems of conservation laws [21] and the H–J equations [18, 20, 8]. The equivalence between the weak, entropy solutions to (1.3) and the viscosity solutions to (1.1) has been known in the literature (see [18, 2, 6, 23]). For completeness and convenience for the reader, we present a simple elementary argument in section 2, in which we will show that, in any space dimensions, the vanishing viscosity limit solution to (1.3) is equivalent to the viscosity solution of (1.1) for convex Hamiltonian H .

Numerous numerical methods have been developed to solve (1.1) (see [7, 1, 19, 5, 6, 26, 27, 28] and the references therein). The designs of most of these front-capturing schemes are strongly guided by the idea of shock-capturing methods for (1.3). For example, the idea of upwind scheme for (1.1), developed by Osher and Sethian [26], is based on the characteristic information on (1.3). Thus it is of considerable interest to understand the numerical transition from (1.3) to (1.1). Of course, if one is interested only in solving (1.1), one will just need to use the characteristic information of (1.3) as a guide to determine the correct “upwind” direction for a stable discretization of (1.1), rather than solve (1.3) directly. However, solving (1.3) itself is an interesting and challenging numerical problem, since it is only weakly hyperbolic. In addition, as our study here finds, the correct numerical transition from (1.3) to (1.1) involves an interesting numerical issue—the correct usage of numerical viscosity, in particular, in higher dimension—is of interest and importance to the shock-capturing community for general systems of conservation laws in high dimensions.

In this article we will address the following two numerical issues. First, given a numerical solution for (1.3), obtained by a shock-capturing method, how can one recover the viscosity solution of (1.1)? Second, what is an appropriate way to discretize the weakly hyperbolic system (1.3)?

Our numerical study, carried out in sections 3 and 4, shows that in order to recover u by numerically integrating (1.3b), special attention needs to be taken to guarantee that (1.3b) is numerically consistent to (1.3a). This is to say that $\mathbf{p} = \nabla u$ needs to be preserved numerically. Such a numerical consistency is not automatically guaranteed, for example, if one integrates (1.3a) and (1.3b) both over the same spatial cell. This will lead to anomalous oscillations in u even if \mathbf{p} looks perfectly normal. Using the analysis introduced by Jin and Liu [13] for the effect of numerical viscosity for one-dimensional (1-D) systems of conservation laws, we show why such a spurious phenomenon appears and give a generic way to fix this. This approach applies in any space dimensions to at least all first- and second-order shock-capturing schemes. This study, as well as the 1-D results of [13], also contributes to a better understanding of the effect of numerical viscosity in higher-space dimensions for a more general system of conservation laws.

It is known that, for a weakly hyperbolic system, shock-capturing methods may face a difficulty achieving the desired order of accuracy [28, 10]. In section 6 we intro-

duce a second-order relaxation scheme for this weakly hyperbolic system, which seems to produce quite satisfactory results, as demonstrated by our numerical examples in section 7.

Relaxation approximation to systems of conservation laws was first introduced by Jin and Xin in [16]. (See also [3, 17, 25] for recent studies.) The idea there is to introduce a relaxation approximation to a system of conservation laws that can generate entropy solution in the zero relaxation limit. It also gives a class of relaxation schemes that are Riemann solver free. The new relaxation approximation introduced here for the H–J equation and its equivalent system of conservation laws, while maintaining the basic advantage of that constructed for general systems of conservation laws in [16], enjoys greater simplicity since here we need only to add one rate equation for any space dimensions, using the special structure of (1.3). The two reasons that such a second-order scheme works well for a weakly hyperbolic system, in our understanding, are the following. First, the first-order relaxation scheme, as the relaxation time approaches zero, is of Lax–Friedrichs type. It is known that the first-order Lax–Friedrichs scheme and its second-order, multidimensional extension produce quite good results for weakly hyperbolic systems [10, 11]. Second, the relaxation system (6.3) is (strongly) hyperbolic. The relaxation scheme is a discretization of this strongly well-posed system, rather than a weakly hyperbolic system. We believe both factors contribute to the good performance of the second-order relaxation scheme for the weakly hyperbolic system (1.3), and further investigation along this line could be promising for more general weakly hyperbolic systems.

We make some concluding remarks in section 8.

2. Remark on the conservation law formulation of the H–J equations.

It is known [18, 22, 6, 2] that for a convex Hamiltonian, the question of entropy solutions in $W^{1,\infty}$ to the Cauchy problem for the H–J equation

$$(2.1) \quad \begin{aligned} \partial_t u + H(\nabla u) &= 0, \\ u(\mathbf{x}, 0) &= u_0(\mathbf{x}) \end{aligned}$$

is equivalent to that of the entropy solutions in L^∞ to the Cauchy problem for the corresponding conservation law

$$(2.2) \quad \begin{aligned} \partial_t \mathbf{p} + \nabla H(\mathbf{p}) &= 0, \\ \mathbf{p}(\mathbf{x}, 0) &= \mathbf{p}_0(\mathbf{x}) = \nabla u_0(\mathbf{x}). \end{aligned}$$

For completeness of the presentation and the convenience of the reader, we will give an elementary argument for such an equivalence. For simplicity, we will assume that $u_0(\mathbf{x})$ is smooth—say, $u_0 \in C^1$.

First, let $u \in W^{1,\infty}$ be the viscosity solution to (2.1). It is straightforward to show that $\mathbf{p} = \nabla u \in L^\infty$ is a weak solution to (2.2). Moreover, \mathbf{p} is the limit of a viscous perturbation of (2.2), i.e., there exists a smooth solution $\mathbf{p}^\epsilon(\mathbf{x}, t)$ to

$$(2.3) \quad \begin{aligned} \partial_t \mathbf{p}^\epsilon + \nabla H(\mathbf{p}^\epsilon) &= \epsilon \Delta \mathbf{p}^\epsilon, \\ \mathbf{p}^\epsilon(\mathbf{x}, 0) &= \nabla u_0(\mathbf{x}), \end{aligned}$$

such that \mathbf{p}^ϵ converges to \mathbf{p} in L^m for any $m < \infty$ and in the weak-* topology in L^∞ .

Indeed, since u is the viscosity solution to (2.1) and H is convex, there exists a smooth solution $u^\epsilon(x, t)$ to

$$(2.4) \quad \begin{aligned} \partial_t u^\epsilon + H(\nabla u^\epsilon) &= \epsilon \Delta u^\epsilon, \\ u^\epsilon(\mathbf{x}, 0) &= u_0(\mathbf{x}), \end{aligned}$$

such that u^ϵ is uniformly bounded in $W^{1,\infty}$, and $u^\epsilon \rightarrow u$ in $W^{1,m}$ (see [18, 19, 22]). Set $\mathbf{p}^\epsilon = \nabla u^\epsilon$, then (2.4) implies (2.3). Denoting by \mathbf{p} the weak-* limit of \mathbf{p}^ϵ in L^∞ , multiplying (2.3) by a test function and integrating by parts, one can show easily that, as $\epsilon \rightarrow 0^+$, \mathbf{p} is a weak solution to (2.2). Thus, by construction, \mathbf{p} is the desired vanishing viscosity limit solution to (2.2).

Conversely, let $\mathbf{p}(\mathbf{x}, t) \in L^\infty$ be a weak solution to (2.2) obtained by the vanishing viscosity method, i.e., (2.3) has smooth solutions \mathbf{p}^ϵ which are uniformly bounded in L^∞ such that

$$(2.5) \quad \mathbf{p}^\epsilon(\mathbf{x}, t) \rightarrow \mathbf{p}(\mathbf{x}, t) \quad \text{in } L^m,$$

and in weak-* topology in L^∞ . Then there exists the unique viscosity solution $u(\mathbf{x}, t)$ to (2.1) satisfying

$$(2.6) \quad \nabla u(\mathbf{x}, t) = \mathbf{p}(\mathbf{x}, t) \quad \text{almost everywhere (a.e.).}$$

Indeed, let $\mathbf{p}^\epsilon(\mathbf{x}, t)$ be the solution to (2.3) satisfying the property (2.5). Let $u^\epsilon(\mathbf{x}, t)$ be the unique solution of

$$(2.7) \quad \begin{aligned} \partial_t u^\epsilon - \epsilon \Delta u^\epsilon &= -H(\mathbf{p}^\epsilon), \\ u^\epsilon(\mathbf{x}, 0) &= u_0(\mathbf{x}). \end{aligned}$$

Problem (2.7) has a global smooth solution $u^\epsilon(x, t)$. Moreover, by the maximal principle and the assumption (2.5), there exists a constant $C = C(T)$ independent of ϵ such that

$$(2.8) \quad |u^\epsilon| \leq C(T) \quad \text{for } 0 < t \leq T.$$

To estimate the derivative of u^ϵ , one may differentiate (2.7) with respect to \mathbf{x} to get

$$(2.9) \quad \begin{aligned} \partial_t(\nabla u^\epsilon) - \epsilon \Delta(\nabla u^\epsilon) &= -\nabla H(\mathbf{p}^\epsilon), \\ \nabla u^\epsilon(\mathbf{x}, 0) &= \nabla u_0(\mathbf{x}). \end{aligned}$$

It follows from (2.3) and (2.9) that

$$(2.10) \quad \begin{aligned} \partial_t(\nabla u^\epsilon - \mathbf{p}^\epsilon) - \epsilon \Delta(\nabla u^\epsilon - \mathbf{p}^\epsilon) &= 0, \\ (\nabla u^\epsilon - \mathbf{p}^\epsilon)(\mathbf{x}, 0) &= 0. \end{aligned}$$

The uniqueness of the Cauchy problem of the heat equation (2.10) now yields

$$(2.11) \quad \nabla u^\epsilon(\mathbf{x}, t) \equiv \mathbf{p}^\epsilon(\mathbf{x}, t).$$

This, together with (2.7), shows

$$(2.12) \quad \begin{aligned} \partial_t u^\epsilon + H(\nabla u^\epsilon) &= \epsilon \Delta u^\epsilon, \\ u^\epsilon(\mathbf{x}, 0) &= u_0(\mathbf{x}). \end{aligned}$$

Moreover, u^ϵ is uniformly bounded in $W^{1,\infty}$. Thus there is a $u \in W^{1,\infty}$ such that

$$(2.13) \quad \begin{aligned} u^\epsilon &\rightarrow u \quad \text{uniformly,} \\ \nabla u^\epsilon &\rightarrow \nabla u \quad \text{in } L^m, \end{aligned}$$

where m is any positive integer less than infinity. It follows from (2.13), (2.11), and (2.5) that

$$(2.14) \quad \mathbf{p}(\mathbf{x}, t) = \nabla u \quad \text{a.e.}$$

Moreover, u is the unique viscosity solution to (2.1) by the classical theory (see [20, 21, 8, 9]).

3. Numerical transition: A 2-D example. Consider the 2-D H–J equation

$$(3.1a) \quad \partial_t u + H(\partial_x u, \partial_y u) = 0,$$

where

$$(3.1b) \quad H(p, q) = \sqrt{1 + p^2 + q^2}$$

is a convex function. The corresponding system of conservation laws is

$$(3.2a) \quad \partial_t p + \partial_x H(p, q) = 0,$$

$$(3.2b) \quad \partial_t q + \partial_y H(p, q) = 0,$$

with

$$(3.2c) \quad \partial_t u + H(p, q) = 0.$$

Integrating over the grid cell $c_{ij} = [x_{i-1/2}, x_{i+1/2}] \times [y_{j-1/2}, y_{j+1/2}]$, one can define the cell average for a generic variable v over c_{ij} by

$$(3.3) \quad v_{ij} = \frac{1}{\Delta x \Delta y} \int_{x_{i-1/2}}^{x_{i+1/2}} \int_{y_{j-1/2}}^{y_{j+1/2}} v(x, y) \, dx dy.$$

Integrating (3.2) over c_{ij} , one gets

$$(3.4a) \quad \partial_t p_{ij} + \frac{1}{\Delta x} (H_{i+1/2,j} - H_{i-1/2,j}) = 0,$$

$$(3.4b) \quad \partial_t q_{ij} + \frac{1}{\Delta y} (H_{i,j+1/2} - H_{i,j-1/2}) = 0,$$

$$(3.4c) \quad \partial_t u_{ij} + H_{ij}(p, q) = 0.$$

To define $H_{ij}(p, q)$ in (3.4c), since

$$(3.5) \quad H_{ij}(p, q) = H(p_{ij}, q_{ij}) + O(\Delta x^2),$$

it is natural to approximate (3.4c) by

$$(3.6) \quad \partial_t u_{ij} + H(p_{ij}, q_{ij}) = 0.$$

We call (3.6) “Scheme I” to distinguish it from “Scheme II, III, and IV” to be introduced in section 4. The only difference among these schemes lies in the integration of (3.2c).

We use the second-order relaxation scheme to be introduced in section 6 to define the numerical flux $H_{i+1/2,j}$ and $H_{i,j+1/2}$ in (3.4a), and then update u by (3.6) using the classical second-order Runge–Kutta method. The numerical phenomenon, as well as the analysis and the remedy, however, is method independent and applies to at least all first- and second-order shock-capturing methods.

We use the following initial data [26]:

$$(3.7) \quad \begin{aligned} u(x, y, 0) &= -.25[\cos(2\pi x) - 1][\cos(2\pi y) - 1] + 1, \\ p(x, y, 0) &= u_x(x, y, 0) = .5\pi \sin(2\pi x)[\cos(2\pi y) - 1], \\ q(x, y, 0) &= u_y(x, y, 0) = .5\pi \sin(2\pi y)[\cos(2\pi x) - 1], \end{aligned}$$

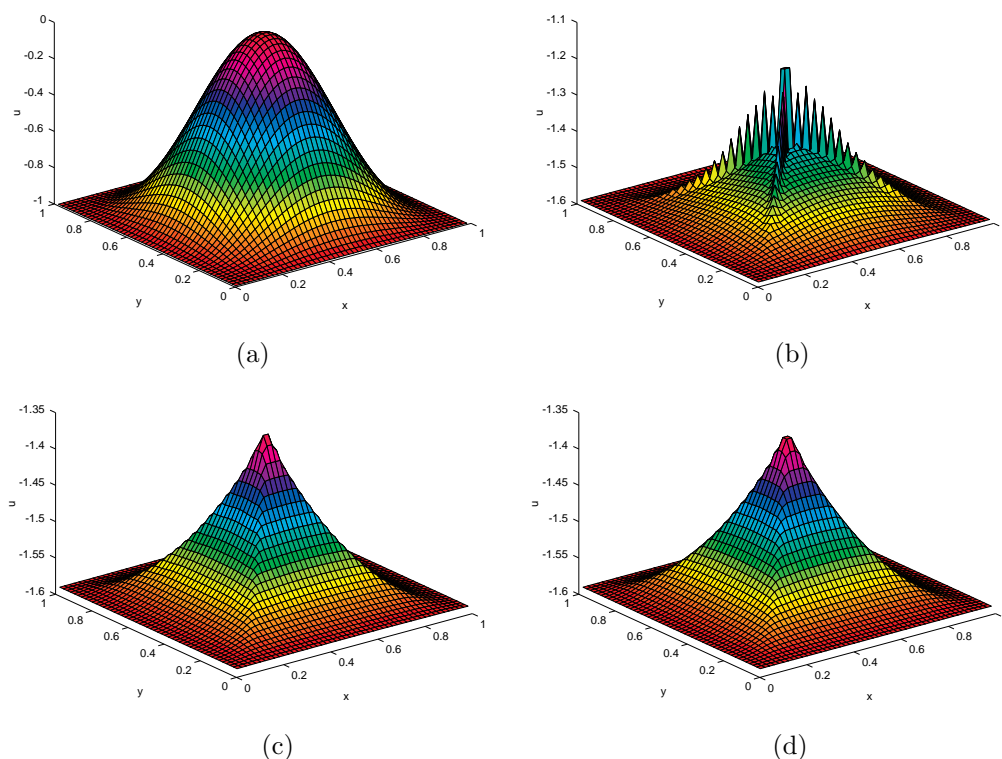


FIG. 3.1. (a) $-u_{ij}$ at $t = 0$. (b) $-u_{ij}$ at $t = 0.6$ by Scheme I. (c) $-u_{i+1/2,j}$ at $t = 0.6$ by Scheme II. (d) $-u_{ij}$ at $t = 0.6$ by Scheme IV.

which gives a flat surface in the boundary of the unit square with a global minimum at $(.5, .5)$. We use $\Delta t = 0.1$ and 50 grid points in each direction and periodic boundary conditions. The viscosity solution for u is a surface with its minimum focusing into a deep dent which opens up. The surface moves upward with unit speed, asymptotically approaching a flat sheet. For a better visualization we plot $-u$ in Fig. 3.1. In Fig. 3.1a the initial profile is displayed. In Fig. 3.1b we plot the numerical solution at $t = 0.6$ by Scheme-I. We also solve the same problem using Scheme II and Scheme IV to be introduced in section 4, which we define as good schemes. One can see from these pictures that Scheme I yields very different results than do the other good schemes. Besides the severe oscillations around the cusp, Scheme I also gives unphysical u even in a smooth region (notice the scaling difference in Fig. 3.1a and Fig. 3.1b). Scheme II and Scheme IV both give the same viscosity solution obtained by Osher and Sethian [26] using a direct solver to (3.1).

In Fig. 3.2 we depict a cross section of p at $t = 0, 0.1, 0.2, 0.3, 0.4, 0.5, 0.6$ for fixed $y = 0.25$. Beginning with a smooth function, p soon develops a shock, and the evolution becomes slower at later times. In Fig. 3.3a we depict $H_{ij} = H(p_{ij}, q_{ij})$ used by Scheme I and $H_{i+1/2,j}$ used by Scheme II and \bar{H}_{ij} .

The H used by Scheme I has two spikes at the two discontinuities of p , while the H used in Schemes II and IV are monotone profiles which differ from the first H only in the spike regions. Such a difference in H , however, leads to a significant difference in u , as shown in Figs. 3.3b and 3.3d.

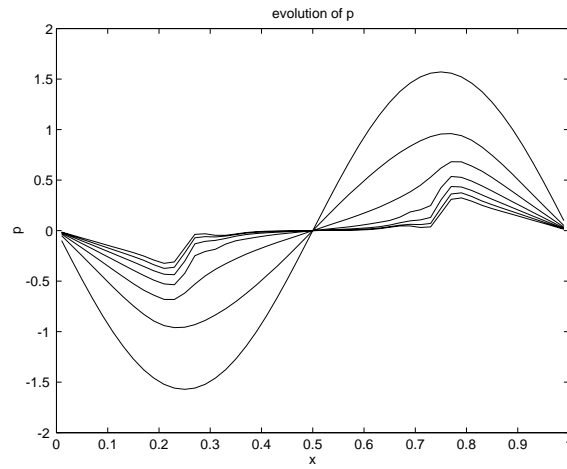


FIG. 3.2. Numerical solution of p at $t = 0, 0.1, 0.2, 0.3, 0.4, 0.5, 0.6$ for fixed $y = 0.25$.

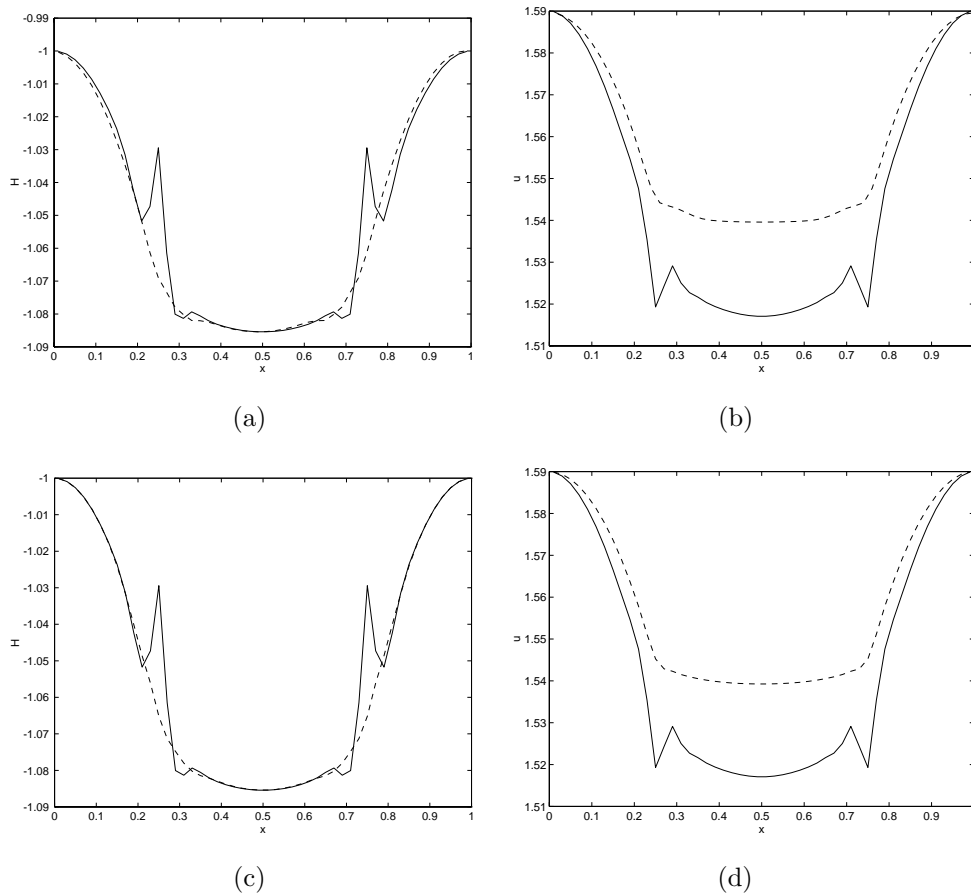


FIG. 3.3. (a) H_{ij} at $t = 0.6$ by solid line and $H_{i+1/2,j}$ at $t = 0.6$ by the dashed line. (b) The solid line is u at $t = 0.6$ by Scheme I, and the dashed line is u at $t = 0.6$ by Scheme II. (c) H_{ij} at $t = 0.6$ by solid line and $\bar{H}_{i,j}$ at $t = 0.6$ by the dashed line. (d) The solid line is u at $t = 0.6$ by Scheme I, and the dashed line is u at $t = 0.6$ by Scheme IV.

In next section we show why the spike in H appears by a traveling wave analysis on a viscous regularization to (3.4a, b), and how one can recover a monotone H . In section 4 we introduce algorithms for (3.4c) (Schemes II, III, and IV), which use the monotone H to solve for u . We show that using such H 's we obtain the viscosity solution of the H–J equation. This study follows the framework of [13], where the effect of numerical viscosity for slowly moving shock in 1-D is examined and similar numerical phenomena resolved.

4. The effect of numerical viscosity.

4.1. An illustrative example. The simplest way to understand the numerical phenomenon reported here is to consider the 1-D inviscid Burger's equation

$$(4.1a) \quad \partial_t u + \partial_x \frac{u^2}{2} = 0,$$

$$(4.1b) \quad u(0, x) = 1 \quad \text{if } x \leq 0.5; \quad u(0, x) = -1 \quad \text{if } 0.5 < x \leq 1.$$

The exact solution to this problem is a stationary shock sitting in the origin, so the solution at later time is always the same as the initial one. This exact solution to $u^2/2$ is $u^2 \equiv 0.5$ for all x . We also use the second order relaxation scheme [16] to solve this problem numerically and display the numerical solutions of u and $u^2/2$ at $t = 0.1$ in Fig. 4.1. While u_i is a monotone profile across the discontinuity, $u_i^2/2$ exhibits a spike at the shock layer of u , which significantly differs from the analytic solution $u^2/2 \equiv 0.5$. We also plot the numerical flux $(U^2/2)_{i+1/2}$, which agrees perfectly with the analytic solution without the spike.

This simple example shows that one should be very careful when using the information in the unphysical shock layer to obtain other physical quantities (such as $u^2/2$ here). When $u^2/2$ is needed it is clearly better to use the numerical flux $(u^2/2)_{i+1/2}$ rather than the cell average value $(u^2/2)_i$.

For nonlinear systems the spike appears for physical quantities, such as the momentum in the Euler equations, when the shock is stationary or moves slowly. For general systems of conservation laws such a phenomenon was studied by Jin and Liu [13], while earlier similar approaches had been taken for specific systems of conservation laws [4, 12, 29]. Here we extend these studies to the 2-D problem and show that the numerical viscosity causes the spike, which can be eliminated using a change of variable. Moreover this analysis also leads to several working schemes that give the correct viscosity solution to the H–J equation.

4.2. The existence of the spike. In order to understand the behavior of the solution obtained by the shock-capturing methods, we study the following viscous system of conservation laws for p and q :

$$(4.2a) \quad \partial_t p + \partial_x H = \epsilon \partial_{xx} p,$$

$$(4.2b) \quad \partial_t q + \partial_y H = \epsilon \partial_{yy} q.$$

This is the modified equation for a linear, first-order scheme such as the Lax–Friedrichs scheme. For nonlinear schemes the numerical viscosity is nonlinear, but similar analysis can also be carried out to study similar numerical phenomena.

To study the behavior for small viscosity ϵ , we look for a planar traveling wave solution to (4.2). First we look for the planar traveling waves moving in the x -direction of the form

$$(4.3) \quad p(x, y, t) = \tilde{p}(\xi), \quad q(x, y, t) = \tilde{q}(\xi)$$

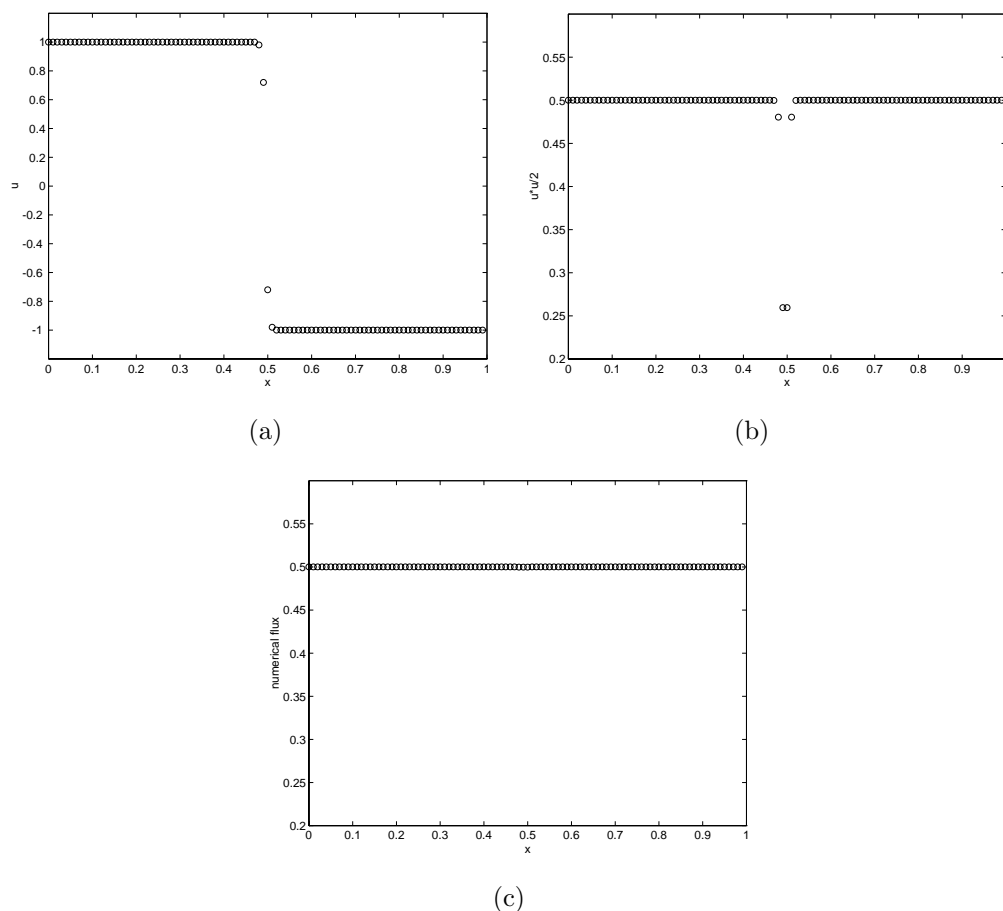


FIG. 4.1. The numerical solution to (3.0) at $t = 0.1$. (a) u ; (b) $u^2/2$; (c) numerical flux.

where $\xi = \frac{x-st}{\epsilon}$, s is the speed of wave (a constant), with asymptotic boundary values at infinities as

$$(4.4) \quad \tilde{p}(\pm\infty) = p_{\pm}, \quad \tilde{q}(\pm\infty) = q_{\pm}.$$

Substituting (4.3) in (4.2) one obtains

$$(4.5a) \quad -s\tilde{p}_{\xi} + H_{\xi}(\tilde{p}(\xi), \tilde{q}(\xi)) = \tilde{p}_{\xi\xi},$$

$$(4.5b) \quad -s\tilde{q}_{\xi} = 0.$$

Thus the problem for $\tilde{q}(\xi)$ becomes

$$(4.6) \quad -s\tilde{q}_{\xi} = 0, \quad \tilde{q}(\pm\infty) = q_{\pm}.$$

Clearly, for any nonstationary wave ($s \neq 0$) the only solution to (4.6) is

$$(4.7) \quad \tilde{q}(\xi) \equiv q_{+} = q_{-} = q_{\pm}.$$

Then the problem for $\tilde{p}(\xi)$ becomes

$$(4.8a) \quad -s\tilde{p}_{\xi} + \partial_{\xi}H(\tilde{p}(\xi), q_{\pm}) = \partial_{\xi\xi}\tilde{p}(\xi),$$

$$(4.8b) \quad \lim_{\xi \rightarrow \pm\infty} \tilde{p}(\xi) = p_{\pm}.$$

This becomes the 1-D scalar equation, so the existence and monotonicity of the solution is guaranteed for the shock wave [21].

Integrating (4.8a) over ξ , one gets

$$(4.9) \quad -s\tilde{p} + H = \tilde{p}_\xi + C,$$

where $C = -sp_- + H(p_-, q_-)$ is the integration constant. Clearly (4.9) shows that

$$(4.10) \quad H = s\tilde{p} + \tilde{p}_\xi + C.$$

Since \tilde{p} is a monotone profile from p_- to p_+ , \tilde{p}_ξ has the spike structure. Equation (4.9) indicates that H is a superposition of a monotone profile $s\tilde{p}$ and a spike \tilde{p}_ξ . When $|s\tilde{p}| \ll |\tilde{p}_\xi|$ (this is particularly the case when the shock speed is small compared to other characteristic speeds), the spike dominates and the solution of H becomes a spike in the ξ direction.

In the case that $s = 0$, (4.5b) has no constraint on $\tilde{q}(\xi)$. (4.5a) becomes

$$\partial_\xi H(\tilde{p}, \tilde{q}) = \tilde{p}_{\xi\xi},$$

which implies

$$(4.11) \quad \partial_\xi \tilde{p} = H(\tilde{p}(\xi), \tilde{q}(\xi)) - H(p_-, q_-)$$

Then the solution is not unique. Thus, we have to be careful with an approximation to (4.2) since it may pick up the wrong solution! However, a natural requirement on the solution of (4.2) is that $p_y = q_x$, which implies $\partial_\xi \tilde{q}(\xi) = 0$, so even in the stationary case one should have $\tilde{q}(\xi) \equiv q_+ = q_-$.

Remark. Instead of (4.2), one may consider the fully regularized problem

$$(4.12a) \quad \partial_t p + \partial_x H = \epsilon \Delta p,$$

$$(4.12b) \quad \partial_t q + \partial_y H = \epsilon \Delta q,$$

where $\Delta = \partial_{xx} + \partial_{yy}$ is the standard Laplacian. Then by repeating our previous analysis, one sees that a planar traveling wave solution of the form (4.3) satisfies

$$(4.13) \quad -s\partial_\xi \tilde{q}(\xi) = \partial_{\xi\xi} \tilde{q}, \quad \lim_{\xi \rightarrow \pm\infty} \tilde{q}(\xi) = q_\pm.$$

Equation (4.13) has a smooth solution if and only if $\tilde{q}(\xi) \equiv q_\pm$ whether $s = 0$ or not. The equation for $\tilde{p}(\xi)$ is now

$$(4.14) \quad -s\partial_\xi \tilde{p}(\xi) + \partial_\xi H(\tilde{p}(\xi), q_\pm) = \partial_{\xi\xi} \tilde{p},$$

$$\lim_{\xi \rightarrow \infty} \tilde{p}(\xi) = p_\pm,$$

which again has a spiky profile for H since integrating (4.14) over ξ gives (4.9).

Since most shock-capturing methods use dimensional splitting, (4.2) is more typical than (4.12).

4.3. Recovering the monotone H . As done in [13] for a 1-D system of conservation law, here we can also recover a monotone H . Note that from (4.10),

$$(4.15) \quad \bar{H} \equiv H - \tilde{p}_\xi = s\tilde{p} + C$$

is a monotone profile. The equivalence of (4.15) for (4.2a) is the change of variable

$$(4.16) \quad \bar{H} = H - \epsilon \partial_x p.$$

Similarly one can also recover a monotone H from (4.2b) using

$$(4.17) \quad \bar{H} = H - \epsilon \partial_y q.$$

5. The working schemes. The traveling wave analysis in section 4 not only explains the source of the spike, which is solely due to the presence of the numerical viscosity, but also shows how to remove the spike: *An analog of the transformation (4.16) or (4.17) should be performed numerically.*

The numerical flux for a general shock-capturing method can be written as

$$(5.1a) \quad H_{i+1/2,j} = \frac{1}{2}(H_{ij} + H_{i+1,j}) - P_{i+1/2,j}\Delta_{i+1/2}p,$$

$$(5.1b) \quad H_{i,j+1/2} = \frac{1}{2}(H_{ij} + H_{i,j+1}) - Q_{i,j+1/2}\Delta_{j+1/2}q,$$

where $\Delta_{j+1/2} \cdot = \cdot_{j+1} - \cdot_j$, and P, Q are the numerical viscosity matrices, which are method specific. We leave P, Q unspecified since this study is general for *all* shock-capturing methods. Applying (5.1) into (3.4a,b) one gets

$$(5.2a) \quad \partial_t p_{ij} + \frac{1}{2\Delta x}(H_{i+1,j} - H_{i-1,j}) = \frac{1}{\Delta x}(P_{i+1/2,j}\Delta_{i+1/2}p - P_{i-1/2,j}\Delta_{i-1/2}p),$$

$$(5.2b) \quad \partial_t q_{ij} + \frac{1}{2\Delta y}(H_{i,j+1} - H_{i,j-1}) = \frac{1}{\Delta y}(Q_{i,j+1/2}\Delta_{j+1/2}q - Q_{i,j-1/2}\Delta_{j-1/2}q).$$

The continuous limit of (5.2) is

$$(5.3a) \quad \partial_t p + \partial_x H(p, q) = \partial_x (P \partial_x p),$$

$$(5.3b) \quad \partial_t q + \partial_y H(p, q) = \partial_y (Q \partial_y q).$$

An analogous transformation of (4.16) for (5.3) is then

$$(5.4) \quad \bar{H} = H - P \partial_x p.$$

The discrete analogue of (5.4) for (5.2a) is

$$(5.5) \quad \bar{H}_{ij} = \frac{1}{2}(H_{ij} + H_{i+1,j}) - P_{i+1/2,j}\Delta_{i+1/2}p.$$

This is a consistent, second-order discretization of (5.4). By comparing (5.5) with (5.1a) one sees that

$$(5.6) \quad \bar{H}_{ij} = H_{i+1/2,j}.$$

Thus the discrete transformation (5.5) simply transfers the cell average value or the value at cell center H_{ij} into the numerical flux in x -direction $H_{i+1/2,j}$!

This defines our recovering of a monotone H . While the cell average H_{ij} has a spike, the numerical flux $H_{i+1/2,j}$ does not have the spike (this is also justified numerically in Figs. 3.3a and 3.3c). This is the quantity to be used to solve for u in (5.2c), instead of (5.6). Thus the Scheme II for u to replace (5.6) should be

$$(5.7) \quad \partial_t u_{i+1/2,j} + H_{i+1/2,j} = 0.$$

Clearly this is also consistent with (3.4a). Since $p = u_x$, (3.4a) is just

$$(5.8) \quad \partial_t \partial_x u_{ij} + \frac{1}{\Delta x}(H_{i+1/2,j} - H_{i-1/2,j}) = 0.$$

If one thinks of $\partial_x u_{ij} = \frac{1}{\Delta x}(u_{i+1/2,j} - u_{i-1/2,j})$, then (5.7) is clearly consistent with (5.8).

A natural question is whether such a u is the viscosity solution to the H–J equation. Using (5.5) and (5.6) in (5.7) one sees that

$$(5.9) \quad \partial_t u_{i+1/2,j} + \frac{1}{2}(H_{ij} + H_{i+1,j}) = P_{i+1/2,j} \Delta_{i+1/2} p = 0.$$

This is consistent with

$$(5.10) \quad \partial_t u + H = \Delta x P \partial_x p = \Delta x P \partial_{xx} u.$$

Thus it selects the viscosity solution with viscosity in the x -direction.

Another working scheme (Scheme III) is to use the numerical flux in the y -direction, $H_{i,j+1/2}$. This will give a way to compute $u_{i,j+1/2}$ as

$$(5.11) \quad \partial_t u_{i,j+1/2} + H_{i,j+1/2} = 0,$$

which selects the viscosity solution u as the limit of

$$(5.12) \quad \partial_t u + H = \Delta y Q \partial_{yy} u.$$

Another reasonable way to define a monotone H is to take the average H

$$(5.13) \quad \bar{\bar{H}}_{ij} = \frac{1}{4}(H_{i+1/2,j} + H_{i-1/2,j} + H_{i,j+1/2} + H_{i,j-1/2})$$

and solve for u_{ij} from

$$(5.14) \quad \partial_t u_{ij} + \bar{\bar{H}}_{ij} = 0.$$

Equation (5.14) is called Scheme IV. Since (5.10) takes numerical fluxes from both x and y directions, it is consistent to the viscosity solution defined by

$$(5.15) \quad \partial_t u + H = \Delta x P \partial_{xx} u + \Delta y Q \partial_{yy} u.$$

In section 3 we showed the numerical results obtained using Scheme II and Scheme IV. Scheme III gives approximately the same results as Scheme II. They all give the correct (and good) viscosity solution. It should be remarked that such an approach is dimension independent and applies to problems in any space dimensions.

Remark. For (1.3a) and (1.3b) to be consistent, \mathbf{p} needs to remain as the gradient of u . Numerically, this property is preserved if the discretization of (3.2c) is consistent with those of (3.2a, b). Scheme II, (5.7), is indeed consistent with (3.4a). Similarly, Scheme III, (5.11), is consistent to (3.4b). This formal argument provides a different perspective on why these schemes should work.

6. A relaxation approximation to the H–J equation.

6.1. A relaxation approximation to the \mathbf{p} -formulation. In this section we introduce a relaxation approximation to the n -dimensional H–J equation

$$(6.1) \quad \partial_t u + H(\nabla u) = 0.$$

This may provide a way to define the weak solution to (6.1). At least in 1-D one can show that our relaxation approximation defines an entropy solution to (6.1) [24, 32].

Let $p_i = \partial_{x_i} u$ ($i = 1, 2, \dots, n$) and $\mathbf{p} = (p_1, p_2, \dots, p_n)$, then \mathbf{p} formally satisfies the following systems of conservation laws:

$$(6.2) \quad \partial_t \mathbf{p} + \nabla H(\mathbf{p}) = 0.$$

We introduce the following hyperbolic system with relaxation:

$$(6.3a) \quad \partial_t \mathbf{p} + \nabla w = 0,$$

$$(6.3b) \quad \partial_t w + a \nabla \cdot \mathbf{p} = -\frac{1}{\epsilon}(w - H(\mathbf{p})),$$

$$(6.3c) \quad \partial_t u + w = 0,$$

where a is a positive constant to be chosen later such that this system is stable. Note that in multiple dimensions this relaxation approximation differs from the original one we proposed in [16] for general systems of conservation laws. Here, to regularize an n -dimensional system of n -equations we just add one additional rate equation (6.3b), due to the special structure of the H–J equation, while in our earlier formulation [16] we need to add n more equations. In 1-D it exactly recovers our original relaxation system for conservation laws.

Comparing with the original system of conservation laws (6.2), the relaxation system (6.3) has several advantages, such as finite speed of propagation, linear convection, and greater regularity. Furthermore, one checks easily that (6.3) is a symmetrizable system in 1-D. Moreover, the relaxation system is (strongly) hyperbolic, while (6.2) is only weakly hyperbolic. This property possibly provides a good framework to design shock-capturing schemes for weakly hyperbolic systems.

To derive a dissipative condition for (6.3), we may apply the Chapman–Enskog expansion to (6.3). By (6.3b),

$$(6.4) \quad w = H(\mathbf{p}) - \epsilon(\partial_t w + a \nabla \cdot \mathbf{p}).$$

Also, (6.3c) gives

$$(6.5) \quad \partial_t \nabla u + \nabla w = 0.$$

Combining (6.5) with (6.3a) gives

$$(6.6) \quad \partial_t(\nabla u - \mathbf{p}) = 0.$$

We take the same initial data so that there is no initial layer,

$$(6.7) \quad \mathbf{p}(\mathbf{x}, 0) = p_0(\mathbf{x}) \equiv \nabla u_0(\mathbf{x}).$$

With (6.7), this implies

$$(6.8) \quad \nabla u(\mathbf{x}, t) = \mathbf{p}(\mathbf{x}, t) \quad \text{for } t \geq 0.$$

Using (6.4),

$$(6.9) \quad w(\mathbf{x}, t) = H(\nabla u) - \epsilon(\partial_t w + a \Delta u).$$

To compute $\partial_t w$, from (6.4),

$$(6.10) \quad \partial_t w = (\nabla_{\mathbf{p}} H(\mathbf{p}))^T \partial_t \mathbf{p} - \epsilon(\partial_{tt} w + a \nabla \cdot \mathbf{p}_t).$$

Using (6.3a),

$$(6.11) \quad \partial_t w = -(\nabla_{\mathbf{p}} H(\mathbf{p}))^T (\nabla w) - \epsilon(\partial_{tt} w + a \nabla \cdot \mathbf{p}_t).$$

Again using (6.4), we get

$$(6.12) \quad \begin{aligned} \nabla w &= \nabla H(\mathbf{p}) - \epsilon(\partial_t \nabla w + a \nabla(\nabla \cdot \mathbf{p})) \\ &= \nabla \mathbf{p} \cdot \nabla_{\mathbf{p}} H - \epsilon(\partial_t \nabla w + a \nabla(\nabla \cdot \mathbf{p})), \end{aligned}$$

where

$$(6.13) \quad \nabla \mathbf{p} = \begin{pmatrix} \partial_{x_1} p_1 & \partial_{x_1} p_2 & \cdots & \partial_{x_1} p_n \\ \partial_{x_2} p_1 & \partial_{x_2} p_2 & \cdots & \partial_{x_2} p_n \\ \cdots & \cdots & \cdots & \cdots \\ \partial_{x_n} p_1 & \partial_{x_n} p_2 & \cdots & \partial_{x_n} p_n \end{pmatrix}, \quad \nabla_{\mathbf{p}} H(\mathbf{p}) = \begin{pmatrix} \partial_{p_1} H \\ \partial_{p_2} H \\ \vdots \\ \partial_{p_n} H \end{pmatrix}.$$

Applying (6.12) in (6.11) gives

$$(6.14) \quad \begin{aligned} \partial_t w &= -(\nabla_{\mathbf{p}} H(\mathbf{p}))^T (\nabla \mathbf{p}) (\nabla_{\mathbf{p}} H(\mathbf{p})) + \epsilon(\nabla_{\mathbf{p}} H(\mathbf{p}))^T (\partial_t \nabla w + a \nabla(\nabla \cdot \mathbf{p})) \\ &\quad - \epsilon(\partial_{tt} w + a \nabla \cdot \mathbf{p}_t). \end{aligned}$$

Finally, using (6.3c), (6.9), and (6.14), we have

$$(6.15) \quad \partial_t u + H(\nabla u) = \epsilon(a \Delta u - (\nabla_{\mathbf{p}} H(\mathbf{p}))^T (\nabla \mathbf{p}) (\nabla_{\mathbf{p}} H(\mathbf{p}))) + O(\epsilon^2).$$

Thus the dissipative condition should be that

$$(6.16) \quad a \Delta u - (\nabla_{\mathbf{p}} H(\mathbf{p}))^T (\nabla \mathbf{p}) \nabla_{\mathbf{p}} H(\mathbf{p}) \quad \text{is an elliptic operator.}$$

Note

$$(6.17) \quad \begin{aligned} &(\nabla_{\mathbf{p}} H(\mathbf{p}))^T (\nabla \mathbf{p}) (\nabla_{\mathbf{p}} H(\mathbf{p})) \\ &= (\partial_{p_1} H, \dots, \partial_{p_n} H) \begin{pmatrix} \partial_{x_1 x_1}^2 u & \partial_{x_1 x_2}^2 u & \cdots & \partial_{x_1 x_n}^2 u \\ \partial_{x_2 x_1}^2 u & \partial_{x_2 x_2}^2 u & \cdots & \partial_{x_2 x_n}^2 u \\ \cdots & \cdots & \cdots & \cdots \\ \partial_{x_n x_1}^2 u & \partial_{x_n x_2}^2 u & \cdots & \partial_{x_n x_n}^2 u \end{pmatrix} \begin{pmatrix} \partial_{p_1} H \\ \partial_{p_2} H \\ \cdots \\ \partial_{p_n} H \end{pmatrix} \\ &= \sum_{ij} (\partial_{p_i} H \partial_{p_j} H) \partial_{x_i x_j}^2 u. \end{aligned}$$

Therefore, the uniform ellipticity requires that

$$(6.18) \quad a \delta_{ij} - \partial_{p_i} H \partial_{p_j} H > 0.$$

That is,

$$(6.19) \quad aI - (\nabla_{\mathbf{p}} H)(\nabla_{\mathbf{p}} H)^T > 0.$$

For any $\xi \in R^n$,

$$(6.20) \quad \begin{aligned} &\xi^t (aI - (\nabla_{\mathbf{p}} H)(\nabla_{\mathbf{p}} H)^T) \xi \\ &= a|\xi|^2 - (\xi_1, \dots, \xi_n) \begin{pmatrix} \partial_{p_1} H \\ \partial_{p_2} H \\ \cdots \\ \partial_{p_n} H \end{pmatrix} (\partial_{p_1} H, \dots, \partial_{p_n} H) \begin{pmatrix} \xi_1 \\ \xi_2 \\ \cdots \\ \xi_n \end{pmatrix} \\ &= (a - |\nabla_{\mathbf{p}} H|^2) |\xi|^2. \end{aligned}$$

Thus the sufficient condition should be

$$(6.21) \quad a > |\nabla_{\mathbf{p}} H|^2.$$

This condition is analogous to the *subcharacteristic condition* for the relaxation approximation for conservation laws [3, 16].

Remark. The equivalent relaxation approximation for the H–J equation (1.1) is clearly

$$(6.22) \quad \begin{aligned} \partial_t u + w &= 0, \\ \partial_t w + a \Delta u &= -\frac{1}{\epsilon}(w - H(\nabla u)). \end{aligned}$$

This is obtained after applying $\mathbf{p} = \nabla u$ in (6.3b). Upon eliminating w this becomes

$$(6.23) \quad \partial_t u + H(\nabla u) = -\epsilon(\partial_{tt} u - a \Delta u),$$

which shows that (6.22) is a perturbation of the H–J equation by a linear wave operator.

6.2. A relaxation scheme. As was done in [16], we can also derive a class of relaxation schemes to the H–J equation based on a discretization of the relaxation approximation (6.3). For example, for a 2-D problem,

$$\begin{aligned} (6.24a) \quad & \partial_t p_1 + \partial_x w = 0, \\ (6.24b) \quad & \partial_t p_2 + \partial_y w = 0, \\ (6.24c) \quad & \partial_t w + a \partial_x p_1 + a \partial_y p_2 = -\frac{1}{\epsilon}(w - H(p_1, p_2)), \\ (6.24d) \quad & \partial_t u + w = 0. \end{aligned}$$

Since (6.24a–c) is a semilinear system of hyperbolic equations, one can easily apply the upwind scheme dimension by dimension. Integrating (6.24a–c) over c_{ij} , we have

$$\begin{aligned} (6.25a) \quad & \partial_t p_{ij}^1 + \frac{1}{\Delta x}(w_{i+1/2,j} - w_{i-1/2,j}) = 0, \\ (6.25b) \quad & \partial_t p_{ij}^2 + \frac{1}{\Delta y}(w_{i,j+1/2} - w_{i,j-1/2}) = 0, \\ (6.25c) \quad & \partial_t w_{ij} + \frac{a}{\Delta x}(p_{i+1/2,j}^1 - p_{i-1/2,j}^1) + \frac{a}{\Delta y}(p_{i,j+1/2}^2 - p_{i,j-1/2}^2) = -\frac{1}{\epsilon}(w_{ij} - H(p_{ij}^1, p_{ij}^2)). \end{aligned}$$

For notation convenience we use $p^1 = p_1, p^2 = p_2$. To define the numerical fluxes we use the second-order upwind scheme (with slope limiter [31]) dimension by dimension. In the x -direction the Riemann invariants are $p^1 \pm \frac{1}{\sqrt{a}}w$, which move with characteristic speeds $\pm\sqrt{a}$; thus the second-order upwind discretization to $p^1 \pm \frac{1}{\sqrt{a}}w$ is

$$(6.26) \quad \begin{aligned} (p^1 + \frac{1}{\sqrt{a}}w)_{i+1/2,j} &= (p^1 + \frac{1}{\sqrt{a}}w)_{ij} + \frac{1}{2}h_j^x \sigma_{ij}^{x,+}, \\ (p^1 - \frac{1}{\sqrt{a}}w)_{i+1/2,j} &= (p^1 - \frac{1}{\sqrt{a}}w)_{i+1,j} - \frac{1}{2}h_{j+1}^x \sigma_{i+1,j}^{x,-}, \end{aligned}$$

where σ_{ij}^\pm are the limited slopes of $p^1 \pm \frac{1}{\sqrt{a}}w$ defined in (6.29), and h_i^x is the mesh size in x direction. This gives

$$\begin{aligned} p_{i+1/2,j}^1 &= \frac{1}{2}(p_{ij}^1 + p_{i+1,j}^1) - \frac{1}{2\sqrt{a}}(w_{i+1,j} - w_{ij}) \\ &\quad + \frac{1}{4}(h_i^x \sigma_{ij}^{x,+} - h_{i+1}^x \sigma_{i+1,j}^{x,-}), \\ w_{i+1/2,j} &= \frac{1}{2}(w_{ij} + w_{i+1,j}) - \frac{\sqrt{a}}{2}(p_{i+1,j}^1 - p_{ij}^1) \\ &\quad + \frac{\sqrt{a}}{4}(h_i^x \sigma_{ij}^{x,+} + h_{i+1}^x \sigma_{i+1,j}^{x,-}). \end{aligned} \quad (6.27)$$

Similarly in the y -direction we have the following numerical fluxes:

$$\begin{aligned} p_{i,j+1/2}^2 &= \frac{1}{2}(p_{ij}^2 + p_{i,j+1}^2) - \frac{1}{2\sqrt{a}}(w_{i,j+1} - w_{ij}) \\ &\quad + \frac{1}{4}(h_j^y \sigma_{ij}^{y,+} - h_{j+1}^y \sigma_{i,j+1}^{y,-}), \\ w_{i,j+1/2} &= \frac{1}{2}(w_{ij} + w_{i,j+1}) - \frac{\sqrt{a}}{2}(p_{i,j+1}^2 - p_{ij}^2) \\ &\quad + \frac{\sqrt{a}}{4}(h_j^y \sigma_{ij}^{y,+} + h_{j+1}^y \sigma_{i,j+1}^{y,-}), \end{aligned} \quad (6.28)$$

where h_j^y is the mesh size in the y -direction. The limited slopes are defined as

$$\begin{aligned} \sigma_{ij}^{x,\pm} &= \frac{1}{h_i^x} \left(p_{i+1,j}^1 \pm \frac{1}{\sqrt{a}} w_{i+1,j} - p_{ij}^1 \mp \frac{1}{\sqrt{a}} w_{ij} \right) \phi(\theta_{ij}^{x,\pm}), \\ \theta_{ij}^{x,\pm} &= \frac{p_{ij}^1 \pm \frac{1}{\sqrt{a}} w_{ij} - p_{i-1,j}^1 \mp \frac{1}{\sqrt{a}} w_{i-1,j}}{p_{i+1,j}^1 \pm \frac{1}{\sqrt{a}} w_{i+1,j} - p_{ij}^1 \mp \frac{1}{\sqrt{a}} w_{ij}}; \\ \sigma_{ij}^{y,\pm} &= \frac{1}{h_j^y} \left(p_{i,j+1}^2 \pm \frac{1}{\sqrt{a}} w_{i,j+1} - p_{ij}^2 \mp \frac{1}{\sqrt{a}} w_{ij} \right) \phi(\theta_{ij}^{y,\pm}), \\ \theta_{ij}^{y,\pm} &= \frac{p_{ij}^2 \pm \frac{1}{\sqrt{a}} w_{ij} - p_{i,j-1}^2 \mp \frac{1}{\sqrt{a}} w_{i,j-1}}{p_{i,j+1}^2 \pm \frac{1}{\sqrt{a}} w_{i,j+1} - p_{ij}^2 \mp \frac{1}{\sqrt{a}} w_{ij}}, \end{aligned} \quad (6.29)$$

with [30]

$$\phi(\theta) = \frac{|\theta| + \theta}{1 + |\theta|}. \quad (6.30)$$

For the time discretization, denote (6.25a–c) by

$$\partial_t U + A(U) = B(U) \quad (6.31)$$

where $A(U)$ stands for the convection terms and $B(U)$ for the relaxation term. Then one can just use a second-order (for $\epsilon \ll \Delta t$) Runge–Kutta-type splitting [16]:

$$U^* = U^n + B(U^n), \quad (6.32a)$$

$$U^{(1)} = U^* - kA(U^*), \quad (6.32b)$$

$$U^{**} = U^{(1)} + B(U^{**}), \quad (6.32c)$$

$$U^{(2)} = U^{**} - kA(U^{**}), \quad (6.32d)$$

$$U^{n+1} = \frac{1}{2}(U^n + U^{(2)}), \quad (6.32e)$$

where k is the time step. Although we use an implicit relaxation term, since the relaxation term is not fully ranked, in (6.32a) and (6.32c) one can always solve for p and q first, using this to update $H(p, q)$, then solve for the unknown w which is linear in both equations. Thus (6.32) can be implemented explicitly.

While for (6.24d), we use the discretization discussed in section 5 for H and then use the classical second-order Runge–Kutta method for time marching. Note for the relaxation scheme we define

$$(6.33) \quad H_{i+1/2,j} = w_{i+1/2,j}, \quad H_{i,j+1/2} = w_{i,j+1/2}.$$

It is known that, for a weakly hyperbolic system, shock-capturing methods in general may have very poor accuracy [28, 10]. However, as demonstrated in next section, our second-order relaxation schemes seem to produce quite satisfactory results. The two reasons, in our understanding, are the following. First, the first-order relaxation scheme, as the relaxation time approaches zero, is of Lax–Friedrichs type. It is known that the first-order Lax–Friedrichs scheme and its second-order, multidimensional sequel produce quite good results for weakly hyperbolic systems [10, 11]. Second, the relaxation system (6.3) is (strongly) hyperbolic. The relaxation scheme is a discretization of this strongly well-posed system, rather than a weakly hyperbolic system. We believe both factors contribute to the good performance of the second-order relaxation scheme for the weakly hyperbolic system (1.3).

7. Numerical examples. In this section we present several numerical examples using the relaxation schemes.

As in [27], we solve the 2-D H–J equation

$$(7.1) \quad \begin{aligned} \partial_t u + H(\partial_x u, \partial_y u) &= 0, \\ u(x, y, 0) &= -\cos \pi \left(\frac{x+y}{2} \right) \end{aligned}$$

in domain $-2 \leq x, y \leq 2$, with a convex H (corresponding to the Burger’s equation in conservation laws),

$$(7.2a) \quad H(u, v) = \frac{1}{2}(u + v + 1)^2,$$

and a nonconvex H ,

$$(7.2b) \quad H(u, v) = \cos(u + v + 1).$$

We use 40 grid points in both x and y directions, and compute to $t = 1.5/\pi^2$. The results are depicted in Fig. 7.1. We also did a convergence study in both l_1 and l_∞ norms at $t = 0.5/\pi^2$, and the results are given in Table 7.1. Due to the large gradient near the local extrema the decay is not quite second order. Similar behavior exists also for the second-order Osher–Sethian method [25] and the essentially nonoscillatory (ENO) schemes in [27]. Notice that the decay rates for the second-order relaxation scheme and the second-order Osher–Sethian scheme are quite comparable, even if the relaxation scheme is based on a weakly hyperbolic system. In the nonconvex case the solution is smoother, and we do observe a second-order convergence in both l_1 and l_∞ norms, as shown in Table 7.2.

In the second example, we take $H(u, v) = \sqrt{u^2 + v^2}$ and the initial condition $u(x, y) = |x| + |y| - 1$. The zero level set of u is a square, centered in the origin, of side

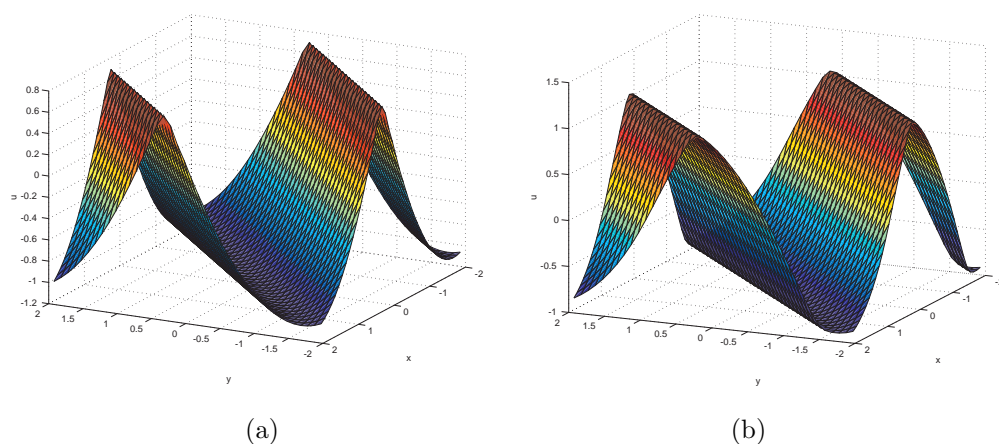


FIG. 7.1. The numerical solutions by the second order relaxation scheme to (7.1) at $t = 1.5/\pi^2$ with: (a) convex H in (7.2a); (b) nonconvex H in (7.2b).

TABLE 7.1
Numerical errors of the convex case (7.2a).

No. Pts.	Relaxation		Osher–Sethian	
	L_1	L_∞	L_1	L_∞
10	0.26811	0.08256	0.21623	0.05743
20	0.05610	0.01916	0.05563	0.02832
40	0.01402	0.00718	0.01573	0.00708
80	0.00344	0.00205	0.00404	0.00189

TABLE 7.2
Numerical errors of the nonconvex case (7.2b).

No. Pts.	Relaxation	
	L_1	L_∞
10	0.18653	0.02560
20	0.04975	0.00788
40	0.01383	0.00197
80	0.00363	0.00050

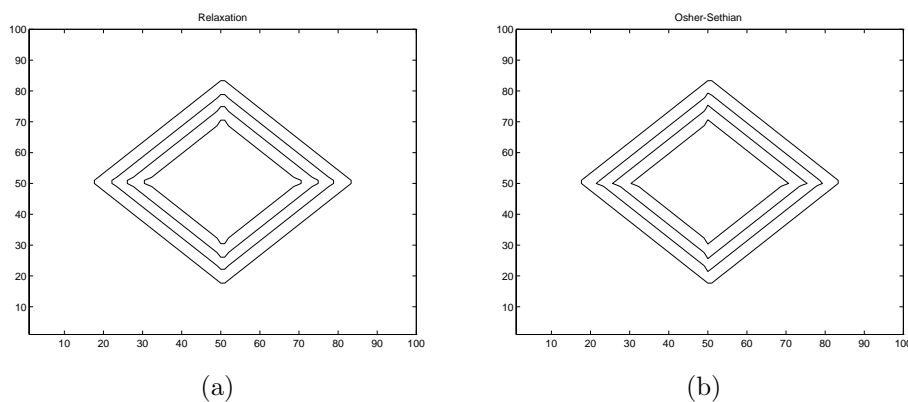


FIG. 7.2. A shrinking diamond: (a) the relaxation scheme, (b) Osher–Sethian scheme. Output time $t = 0, 0.1, 0.2, 0.3$.

length $\sqrt{2}$. We define $p = \text{sign} x$ and $q = \text{sign} y$. This H–J equation describes a solution u whose zero level set (the diamond) moves in the inward normal direction with speed one [26]. The four corners of u correspond to the shocks in p and q . We use 100 grid points between -1.5 and 1.5 in both the x and the y directions. The results given by the second-order relaxation schemes and the second-order Osher–Sethian scheme [26] are depicted in Fig. 7.2. It shows that both schemes give comparable results, although the solution of the Osher–Sethian scheme is slightly sharper.

8. Conclusion. In this article we have studied the numerical transition from a system of conservation laws to an H–J equation. We investigate how to numerically bridge the equivalence of the viscosity solution to the system of conservation laws and that of the corresponding H–J equation. Our study shows that the numerical solution to the system of conservation laws generated by a shock-capturing method should be used carefully in order to convert to the viscosity solution of the H–J equation. In order to achieve this we analyze the structure of the two-dimensional shock profile and find a way to produce the desired viscosity solution correctly. This gives a natural way, in the discrete setting, to maintain the system of conservation laws as the gradient of the H–J equation. Such a study has an impact even beyond the scope of the H–J equation, since a good understanding of the effect of numerical viscosity is a central issue toward a good understanding of the higher-dimensional shock capturing methods.

We then constructed a relaxation approximation to the system of conservation laws and the corresponding H–J equation. This new relaxation approximation, while sharing the spirit of the original one we proposed in [16] for a general system of conservation laws, enjoys a greater simplicity thanks to the special structure of the H–J equation. Numerical results show that it is adequate to use it to solve a weakly hyperbolic system. This issue deserves further investigation for more general weakly hyperbolic systems.

Recently, it was observed in [14] that, when the subcharacteristic condition (6.21) is at the degenerated case (the equality holds), the $O(\epsilon)$ term in the Chapman–Enskog expansion of the relaxation approximation (6.3) becomes the mean-curvature term for a suitable choice of the Hamiltonian. Thus this relaxation system yields asymptotically the level set equation of Osher–Sethian [26] for front propagating in the normal direction with speed $V = 1 - \epsilon\kappa$, where κ is the mean curvature. More detailed analysis, as well as its impact on numerical approximation to such a motion, is carried out in [15].

REFERENCES

- [1] M. BARDI AND S. OSHER, *The nonconvex multidimensional Riemann problem for Hamilton–Jacobi equations*, SIAM J. Math. Anal., 22 (1991), pp. 344–351.
- [2] V. CASELLES, *Scalar conservation laws and Hamilton–Jacobi equations in one-space variable*, Nonlinear Anal., 18 (1992), pp. 461–469.
- [3] G.-Q. CHEN, C.D. LEVERMORE, AND T.P. LIU, *Hyperbolic conservation laws with stiff relaxation terms and entropy*, Comm. Pure Appl. Math., 47 (1993), pp. 787–830.
- [4] B. COCKBURN AND H. GAU, *A model numerical scheme for the propagation phase transitions in solids*, SIAM J. Sci. Comput., 17 (1996), pp. 1092–1121.
- [5] L. CORRIAS, *Fast Legendre–Fenchel transform and applications to Hamilton–Jacobi equations and conservation laws*, SIAM J. Numer. Anal., 33 (1996), pp. 1534–1558.
- [6] L. CORRIAS, M. FALCONE, AND R. NATALINI, *Numerical schemes for conservation laws via Hamilton–Jacobi equations*, Math. Comp., 64 (1995), pp. 555–580.
- [7] M.G. CRANDALL AND P.L. LIONS, *Two approximations of solutions of Hamilton–Jacobi equations*, Math. Comp., 43 (1984), pp. 1–19.

- [8] M. CRANDALL AND P.L. LIONS, *Viscosity solutions of Hamilton-Jacobi equations*, Trans. Amer. Math. Soc., 277 (1983), pp. 1–42.
- [9] M. CRANDALL, L.C. EVANS, AND P.L. LIONS, *Some properties of viscosity solutions to Hamilton-Jacobi equations*, Trans. Amer. Math. Soc., 282 (1984), pp. 487–502.
- [10] BJÖRN ENGQUIST AND O. RUNBORG, *Multi-phase computations in geometrical optics*, J. Comp. Appl. Math., 74 (1996), pp. 175–192.
- [11] G.-S. JIANG AND E. TADMOR, *Nonoscillatory Central Schemes for Multidimensional Hyperbolic Conservation Laws*, SIAM J. Sci. Comput., to appear.
- [12] S. JIN, *Numerical integrations of systems of conservation laws of mixed type*, SIAM J. Appl. Math., 55 (1995), pp. 1536–1551.
- [13] S. JIN AND J.G. LIU, *The effects of numerical viscosities I: Slowly moving shocks*, J. Comp. Phys., 126 (1996), pp. 373–389.
- [14] S. JIN AND M.A. KATSOUKAKIS, *Relaxation approximations to front propagation*, J. Differential Equations, 138 (1997), pp. 380–387.
- [15] S. JIN, M.A. KATSOUKAKIS AND Z.P. XIN, *Relaxation schemes for curvature-dependent front propagation*, Comm. Pure Appl. Math., submitted.
- [16] S. JIN AND Z.P. XIN, *The relaxation schemes for systems of hyperbolic conservation laws in arbitrary space dimensions*, Comm. Pure Appl. Math., 48 (1995), pp. 235–276.
- [17] M.A. KATSOUKAKIS AND A.E. TZAVARAS, *Contractive relaxation systems and the scalar multidimensional conservation laws*, Comm. Partial Differential Equations, 22 (1997), pp. 195–223.
- [18] S.N. KRUKOV, *Generalized solutions of nonlinear first-order equations with several independent variables*, II, Math. USSR-Sb., 1 (1967), pp. 93–116.
- [19] S.N. KRUKOV, *The method of finite differences for a first-order nonlinear equation with many independent variables*, USSR Comp. Math. Phys., 6 (1966), pp. 136–151.
- [20] S.N. KRUKOV, *Generalized solutions to the Hamilton-Jacobi equations of Eikonal type*, I, Math. USSR-Sb., 27 (1975), pp. 406–446.
- [21] P.D. LAX, *Hyperbolic Systems of Conservation Laws and the Mathematical Theory of Shock Waves*, CBMS-NSF Regional Conf. Ser. in Appl. Math. 11, SIAM, Philadelphia, 1973.
- [22] P.L. LIONS, *Generalized solutions of Hamilton-Jacobi equations*, Pitman Res. Notes Math. Ser. 69, Longman, Harlow, UK, 1982.
- [23] P.L. LIONS, AND P.E. SOUGANIDIS, *Convergence of MUSCL and filtered schemes for scalar conservation laws and Hamilton-Jacobi equations*, Numer. Math., 69 (1995), pp. 441–470.
- [24] R. NATALINI, *Convergence to equilibrium for the relaxation approximations of conservation laws*, Comm. Pure Appl. Math., 49 (1996), pp. 795–823.
- [25] R. NATALINI, *A Discrete Kinetic Approximation of Entropy Solutions to Multidimensional Scalar Conservation Laws*, J. Differential Equations, to appear.
- [26] S. OSHER AND J.A. SETHIAN, *Fronts propagating with curvature dependent speed: algorithms based on Hamilton-Jacobi formulations*, J. Comput. Phys., 78 (1988), pp. 12–49.
- [27] S. OSHER AND W. WHITLOW, JR., *Entropy condition satisfying approximations for the full potential equations of transonic flow*, Math. Comp., 44 (1985), pp. 1–29.
- [28] S. OSHER AND C.W. SHU, *High-order essentially nonoscillatory schemes for Hamilton-Jacobi equations*, SIAM J. Numer. Anal., 28 (1991), pp. 907–922.
- [29] M. SLEMROD, *Continuum dynamics of first-order phase transitions*, in Phase Transitions and Material Instabilities in Solids, M. Gurtin, ed., Academic Press, London, 1984, pp. 163–204.
- [30] P.K. SWEBY, *High resolution schemes using flux limiters for hyperbolic conservation laws*, SIAM J. Numer. Anal., 21 (1984), pp. 995–1012.
- [31] B. VAN LEER, *Towards the ultimate conservative difference schemes V. A second-order sequel to Godunov's method*, J. Comp. Phys., 32 (1979), pp. 101–136.
- [32] W.C. WANG AND Z.P. XIN, *On the asymptotic limit of the initial boundary value problem of 1-D scalar conservation laws with relaxation extension*, Comm. Pure Appl. Math., 51 (1998), pp. 505–535.